LV-CONTROL OF A HIGH-PURITY DISTILLATION COLUMN

SIGURD SKOGESTAD[†] and MANFRED MORARI
California Institute of Technology, Chemical Engineering, 206-41, Pasadena, CA 91125, U.S.A.

Abstract—A realistic study of the LV-control of a high-purity distillation column is presented. Linear controllers designed based on a linearized model of the plant are found to yield acceptable performance also when there is model–plant mismatch. The mismatch can be caused by uncertainty on the manipulated inputs, nonlinearity and variations in reboiler and condenser holdup. The presence of input uncertainty makes the use of a steady-state decoupler unacceptable. The effect of nonlinearity is strongly reduced by using the logarithm of the compositions. A simple diagonal PI-controller is not sensitive to model–plant mismatch, but yields a response with a sluggish return to steady-state.

1. INTRODUCTION

In this paper we study the high-purity distillation column in Table 1 using reflux (L) and boilup (V) as manipulated inputs to control the top (y_D) and bottom (x_B) compositions. This column was analyzed previously by the authors (Skogestad and Morari, 1986), but the objective of that previous paper was to study general properties of ill-conditioned plants rather than to study distillation column control which is the objective of this paper. The LV-configuration is chosen because this is the choice of manipulated inputs most commonly used in industrial practice. This does not necessarily mean that this is the best configuration, and, for example, the $(L/D)(V/B)$-configuration may be preferable (Shinskey, 1984; Skogestad and Morari, 1987c).

The distillation column used in this paper was chosen to be representative of a large class of moderately high-purity distillation columns. The goal of this paper is to provide a realistic control design and simulation study for the column (Fig. 1). To be realistic at least the issues of (1) uncertainty and (2) nonlinearity must be addressed.

1.1. *Uncertainty*

Skogestad and Morari (1986) showed that the closed-loop system may be extremely sensitive to input uncertainty when the LV-configuration is used. In particular, inverse-based controllers were found to display severe robustness problems. Therefore, in this paper the uncertainty is explicitly taken into account when designing and analyzing the controllers by using the Structured Singular Value (μ) introduced by Doyle (1982). We also find that μ provides a much easier way of comparing and analyzing the effect of various combinations of controllers, uncertainty and disturbances than the traditional simulation approach.

1.2. *Nonlinearity*

High-purity distillation columns are known to be strongly nonlinear (e.g. Moczek *et al.*, 1963; Fuentes and Luyben, 1983), and any realistic study should take this into account. Our approach is to base the controller design on a linear model. The effect of nonlinearity is taken care of by analyzing this controller for linearized models at *different operating points*. Furthermore, all simulations are based on the full nonlinear model.

1.3. *Logarithmic compositions*

The linear model in terms of unscaled compositions, y_D and x_B, is

$$\begin{pmatrix} \mathrm{d}y_D \\ \mathrm{d}x_B \end{pmatrix} = G(s) \begin{pmatrix} \mathrm{d}L \\ \mathrm{d}V \end{pmatrix} \tag{1}$$

However, all plant models and controllers in this paper are in terms of scaled compositions

$$y_D^S = \frac{y_D}{1 - y_D^o}, \quad x_B^S = \frac{x_B}{x_B^o}. \tag{2}$$

Here x_B^o and $1 - y_D^o$ are the amounts of impurity in each product at the nominal operating print. The scaled plant, G^S, is defined by

$$\begin{pmatrix} \mathrm{d}y_D^S \\ \mathrm{d}x_B^S \end{pmatrix} = G^S \begin{pmatrix} \mathrm{d}L \\ \mathrm{d}V \end{pmatrix}, \quad G^S = \begin{pmatrix} \dfrac{1}{1 - y_D^o} & 0 \\ 0 & \dfrac{1}{x_B^o} \end{pmatrix} G. \tag{3}$$

The relative scaling in eq. 2 is automatically obtained by using logarithmic compositions

$$Y_D = \ln(1 - y_D) \tag{3}$$

$$X_B = \ln x_B$$

because

$$\mathrm{d}Y_D = -\frac{\mathrm{d}y_D}{1 - y_D}, \quad \mathrm{d}X_B = \frac{\mathrm{d}x_B}{x_B}. \tag{4}$$

[†]Presently: Chemical Engineering, Norwegian Institute of Technology (NTH), N-7034 Trondheim, Norway.

Table 1. Steady-state data for distillation column at operating points A and C

Binary separation, constant molar flows, feed liquid

Column data:

Relative volatility	$\alpha = 1.5$
No. of theoretical trays	$N = 40$
Feed tray (1 = reboiler)	$N_F = 21$
Feed composition	$z_F = 0.5$

Operating variables:

	A	C
$y_D =$	0.99	0.90
$x_B =$	0.01	0.002
$D/F =$	0.500	0.555
$L/F =$	2.706	2.737

Steady-state gains (unscaled compositions):

$$\begin{pmatrix} \mathrm{d}y_D \\ \mathrm{d}x_B \end{pmatrix} = G(0) \begin{pmatrix} \mathrm{d}L/F \\ \mathrm{d}V/F \end{pmatrix}$$

$$G(0) = \overset{A}{\begin{pmatrix} 0.878 & -0.864 \\ 1.082 & -1.096 \end{pmatrix}} \overset{C}{\begin{pmatrix} 1.604 & -1.602 \\ 0.01865 & -0.02148 \end{pmatrix}}$$
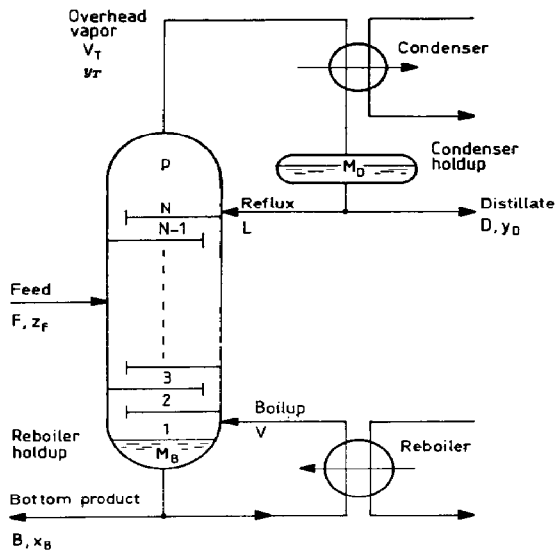
Fig. 1. Two product distillation column with single feed and total condenser.

Ryskamp (1981) has suggested that the use of logarithmic compositions (Y_D and X_B) may reduce the effect of nonlinearity. This has also been confirmed more recently by Skogestad and Morari. They found that the use of logarithmic compositions effectively eliminates the effect of nonlinearity at high frequency (Skogestad and Morari, 1987a) and also reduces its effect at steady-state (Skogestad and Morari, 1987b). For control purposes the high frequency behavior (initial response) is of principal importance. Consequently, if logarithmic compositions are used we expect a linear controller

to perform satisfactorily when we are also far removed from the nominal operating point for which the controller was designed. Another objective of this paper is to confirm that this is indeed true.

In most cases the column is operated close to its nominal operating point and there is hardly any advantage in using logarithmic compositions which in this case merely corresponds to a rescaling of the outputs. However, if, for some reason, the column is taken far from this nominal operating point, for example, during startup or due to a temporary loss of control, the use of logarithmic compositions may bring the column safely back to its nominal operating point, whereas a controller based on unscaled compositions (y_D and x_B) may easily yield an unstable response.

1.4. *Choice of nominal operating point*

The design approach suggested by the above discussion is to design a linear controller based on a linearized model for some nominal operating point. What operating point should be used? If an operating point corresponding to both products of high and equal purities is chosen (i.e. $1 - y_D = x_B$ is small), it is easily shown (Skogestad and Morari, 1987a, b; Kapoor *et al.*, 1986) that the values of the steady-state gains and the linearized time constant will change drastically for small perturbations from this operating point. We may therefore question if acceptable closed-loop control can be obtained by basing the controller design on a linearized model at such an operating point. Kapoor *et al.* (1986) indicate that this is not advisable and that a model based on a perturbed operating point should be used. However, as we just discussed, the high-frequency behavior, which is of primary importance for feedback control, shows much less variation with operating conditions. Therefore, *provided* the model gives a good description of the high-frequency behavior, we also expect to be able to design an acceptable controller when the nominal point has both products of high purity. This is also confirmed by the results in this paper.

A main conclusion of this paper is therefore that acceptable closed-loop performance may be obtained by designing a linear controller based on a linear model at *any* nominal operating point. If large perturbations from steady state are expected then logarithmic compositions should be used to reduce the effect of nonlinearity.

2. THE DISTILLATION COLUMN

Steady-state data for the distillation column are given in Table 1. The following simplifying assumptions are made: (a1) binary separation, (a2) constant relative volatility, (a3) constant molar flows and (a4) constant holdups on all trays and perfect level control. The last assumption results in immediate flow response, that is, we are neglecting flow dynamics. This is somewhat unrealistic and in order to avoid unrealistic controllers, we will add "uncertainty" at high frequency to include the effect of neglected flow

dynamics when designing and analyzing the controllers (see Section 3).

We investigate the column at two different operating points. At the nominal operating point, A, both products are high-purity and $1 - y_D^o = x_B^o = 0.01$. Operating point C is obtained by increasing D/F from 0.500 to 0.555 which yields a less pure top product and a purer bottom product; $1 - y_{DC}^o = 0.10$ and $x_{BC}^o = 0.002$ (subscript C denotes operating point C while no subscript denotes operating point A). We will study the column for the following three assumptions regarding reboiler and condenser holdup

Case 1: Almost negligible condenser and reboiler holdup ($M_D/F = M_B/F = 0.5$ min).

Case 2: Large condenser and reboiler holdup ($M_D/F = 32.1$ min, $M_B/F = 11$ min).

Case 3: Same holdup as in Case 2, but the composition of the overhead vapor (y_T) is used as a controlled output instead of the composition in the condenser (y_D).

These three cases will be denoted by subscript 1, 2 and 3, respectively. The holdup on each tray inside the column is $M_i/F = 0.5$ min in all three cases.

2.1. Modelling

Nominal operating point (A). A 41st order linear model for the columns is easily derived based on the data given in Table 1 (see Skogestad and Morari, 1987a)

$$\begin{pmatrix} \mathrm{d}y_D \\ \mathrm{d}x_B \end{pmatrix} = G(s) \begin{pmatrix} \mathrm{d}L \\ \mathrm{d}V \end{pmatrix}. \tag{5}$$

The scaled steady-state gain matrix is

$$G^S(0) = \begin{pmatrix} 87.8 & -86.4 \\ 108.2 & -109.6 \end{pmatrix} \tag{6}$$

which yields the following values for the condition number and the 1,1-element in the RGA

$\gamma(G^S(0)) = \bar{\sigma}(G^S(0))/\underline{\sigma}(G^S(0)) = 141.7$ $\lambda_{11}(G^S(0)) = 35.1$.

However, $\gamma(G^S)$ and $\lambda_{11}(G^S)$ are much smaller at high frequencies as seen from Fig. 2.

Case 0: A very crude model of the column was presented by Skogestad and Morari (1986) (time in min)

$$\text{Model 0:} \quad G_0(s) = \frac{1}{1 + 75s} G(0). \tag{7}$$

This model gives the same values of $\gamma(G)$ and $\lambda_{11}(G)$ at all frequencies, and is therefore a poor description of the actual plant at high frequency. In our previous study (Skogestad and Morari, 1986) the controller design was based on this simplified model, and one objective of this paper is to study how these controllers perform when a more realistic model is used.

Case 1: For the case of negligible reboiler and condenser holdup the following simple two time-
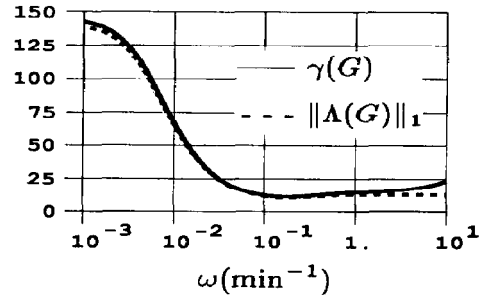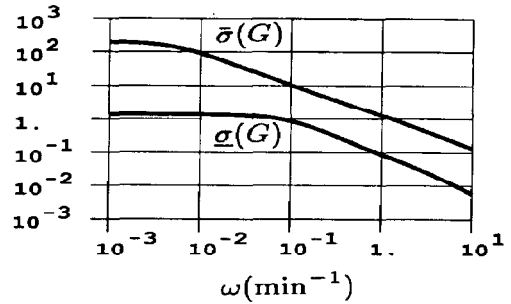
Fig. 2. Column A, Case 1 ($G = G_1^S$). The condition number of the plant is about 10 times lower at high frequencies than at steady state.

constant model yields an *excellent* approximation of the 41st order linear model (Skogestad and Morari, 1987a).

$$G_1^S(s) = \begin{pmatrix} \dfrac{87.8}{1 + \tau_1 s} & -\dfrac{87.8}{1 + \tau_1 s} + \dfrac{1.4}{1 + \tau_2 s} \\ \dfrac{108.2}{1 + \tau_1 s} & -\dfrac{108.2}{1 + \tau_1 s} - \dfrac{1.4}{1 + \tau_2 s} \end{pmatrix} \tag{8}$$

with $\tau_1 = 194$ min and $\tau_2 = 15$ min.

This model has only two states as seen from the minimal realization in the Appendix. $G_1(s)$ uses two time constants: τ_1 is the time constant for changes in the external flows. It corresponds to the dominant time constant and may be estimated, for example, by using the inventory time constant of Moczek *et al.* (1963). τ_2 is the time constant for changes in internal flows (simultaneous change in L and V with constant product rates, D and B) and can be estimated by matching the high-frequency behavior as shown by Skogestad and Morari (1987a). The simple model (8) matches the observed variation in condition number with frequency (Fig. 2).

Cases 2 and 3: The effect of the reboiler and condenser holdups (Case 2) can be partially accounted for by multiplying $G_1(s)$ by diag $\{(1 + \tau_D s)^{-1}, (1 + \tau_B s)^{-1}\}$, where in our case $\tau_D = M_D/V_T = 10$ min and $\tau_B = M_B/L_B = 3$ min. However, sometimes the top composition is measured in the overhead vapor line (Case 3), rather than in the condenser. $G_1(s)$ provides a good approximation of the plant in such cases.

In order to obtain a better low-order model for Case 2 and 3, we performed a model reduction [Balanced Realization, Moore (1981)] on the full 41st order model. A good approximation was obtained with a 5th order model as illustrated in Fig. 3. The state-space realizations of these models [$G_2^S(s)$ and $G_3^S(s)$] are given in Appendix.

Operating point C. We will return with a discussion of the model for this case in Section 6 when we also discuss the control of this plant.

2.2. *Simulations*

The design and analysis of the controller are based on the linear models $G_1(s)$, $G_2(s)$ and $G_3(s)$. However, except for the four simplifying assumptions a1–a4 stated above, all simulations are carried out with the full *nonlinear* model. (In some cases the changes are so small, however, that the results are equivalent to linear simulations.) To get a realistic evaluation of the controllers, *input uncertainty* must be included (Skogestad and Morari, 1986, 1987d). Simulations are therefore shown both with and without 20% uncertainty with respect to the change of the two inputs. The following uncertainties are used

$$\Delta L = (1 + \Delta_1)\Delta L_c, \quad \Delta_1 = 0.2$$

$$\Delta V = (1 + \Delta_2)\Delta V_c, \quad \Delta_2 = -0.2 \qquad (9)$$

Here ΔL and ΔV are the actual changes in manipulated flow rates, while ΔL_c and ΔV_c are the desired values as computed by the controller. $\Delta_1 = -\Delta_2$ was chosen to represent the worst combination of the uncertainties (Skogestad and Morari, 1986, 1987d).

3. CONTROL THEORY

3.1. *Robust performance and robust stability*

The objective of using feedback control is to keep the controlled outputs (in our case y_D and x_B) "close" to their desired setpoints. What is meant by "close" is more precisely defined by the performance specifications. These performance requirements should be satisfied in spite of unmeasured disturbances and
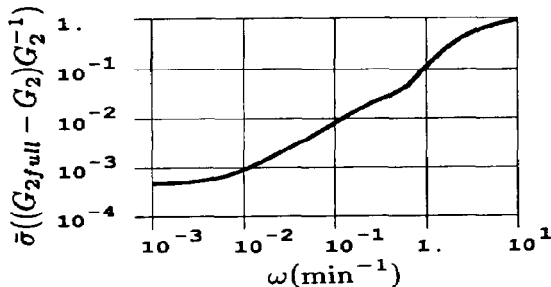
Fig. 3. Column *A*, Case 2. Relative difference between the 5th order model $G_2(s)$ (Appendix) and the 41st order plant $G_{2full}(s)$. The 5th order model provides an excellent approximation within the frequency range of interest ($\omega < 1$ min^{-1}).

model–plant mismatch (uncertainty). Consequently, the ultimate goal of the controller design is to achieve Robust Performance (RP): The performance specification should be satisfied for the *worst case* combination of disturbances and model–plant mismatch.

To check for RP we will use the Structured Singular Value μ (Doyle, 1982). μ of a matrix N (denoted $\mu(N)$ or $\mu_\Delta(N)$) is equal to $1/\bar{\sigma}(\Delta)$ where $\bar{\sigma}(\Delta)$ is the magnitude of the smallest perturbation needed to make the matrix ($I + \Delta N$) singular. $\mu(N)$ depends both on the matrix N and of the *structure* (e.g. diagonal or full matrix) of the perturbation Δ.

As stated, achieving robust performance is the overall goal. The implications of this requirement are easier to understand if we consider some subobjectives which have to be satisfied in order to achieve this goal:

Nominal Stability (NS). The model is assumed to be a reasonable approximation of the true plant. Therefore the closed loop system with the controller applied to the (nominal) plant model has to be stable.

Nominal Performance (NP). In addition to stability, the quality of the response should satisfy some minimum requirements—at least when the controller is applied to the plant model. We will define performance in terms of the weighted H^∞-norm of the closed-loop transfer function S.

$$NP \Leftrightarrow \bar{\sigma}(w_P S) \leqslant 1 \ \forall \omega, S = (I + GC)^{-1}. \quad (10)$$

This is a generalization of classical frequency domain specifications to multi-variable systems. Perfect disturbance rejection is obtained when $S = 0$.

The weight w_P is used to specify the frequency range over which the output errors are to be small. To get consistency with the notation used below define $\bar{\sigma}(w_P S) = \mu(N_{NP})$ such that (10) becomes

$$NP \Leftrightarrow \mu(N_{NP}) \leqslant 1 \ \forall \omega \qquad (11)$$

where $N_{NP} = w_P S$, and μ is computed with respect to the structure of a "full" matrix Δ_P.

Robust Stability (RS). The closed loop system must remain stable for all possible plants as defined by the uncertainty description. For example, assume there is uncertainty with respect to the actual magnitude of the manipulated inputs (which is always the case!). The perturbed plants, G_p, are then given by

$$G_p = G(I + \Delta_I), \quad \Delta_I = \begin{pmatrix} \Delta_1 & 0 \\ 0 & \Delta_2 \end{pmatrix} \qquad (12)$$

where $\Delta_i(s)$ is the relative uncertainty for input i. We will consider the case when the magnitude of this uncertainty is equal for both inputs

$$|\Delta_i| \leqslant |w_I(jw)|, \quad i = 1, 2. \qquad (13)$$

The robust stability requirement can be checked using μ. In this particular case (Skogestad and Morari, 1986)

$$RS \Leftrightarrow \mu(N_{RS}) \leqslant 1, \ \forall \omega \qquad (14)$$

where $N_{RS} = w_I CGS$ and μ is computed with respect to the diagonal 2×2 matrix Δ_I.

Robust Performance (RP). The closed loop system must satisfy the performance requirements for all possible plants as defined by the uncertainty description. As an example we may require (10) to be satisfied when G is replaced by any of the possible perturbed plants G_p as defined by the uncertainty description (12).

$$RP \Leftrightarrow \bar{\sigma}(w_P(I + G_pC)^{-1}) \leqslant 1 \quad \forall \omega, \; \forall G_p. \quad (15)$$

This definition of Robust Performance is of no value without a simple method to test if condition (15) is satisfied for all possible perturbed plants G_p generated by (12) and (13). Again it turns out that the structured singular value μ gives a condition which is relatively easy to check:

$$RP \Leftrightarrow \mu(N_{RP}) \leqslant 1, \quad \forall \omega \quad (16a)$$

where

$$N_{RP} = \begin{pmatrix} w_I CSG & w_I CS \\ w_P SG & w_P S \end{pmatrix} \quad (16b)$$

and μ is computed with respect to the structure diag $\{\Delta_I, \Delta_p\}$ where Δ_I is 2×2 diagonal matrix and Δ_P is a full 2×2 matrix.

3.2. *The RGA*

Let $\times$ denote element-by-element multiplication. The RGA of the matrix G (Bristol, 1966) is defined as

$$\Lambda(G) = G \times (G^{-1})^T. \quad (17)$$

The RGA is *independent* of input and output scaling. The RGA of the *plant* is commonly used as a tool for selecting control configurations for distillation columns (Shinskey, 1984). However, in this paper we will make use of the RGA of the *controller* as a measure of a system's sensitivity to input uncertainty (Skogestad and Morari, 1987d). Before stating this result, we will point out the close relationship between large plant RGA-elements and a high condition number. The condition number of the plant is $\gamma(G) = \bar{\sigma}(G)/\underline{\sigma}(G)$ which is the ratio between the plant's maximum and minimum gain (see Notation). A plant with a large value of $\gamma(G)$ is "ill-conditioned" and has a strong "directionality" since the plant gain depends strongly on the input direction. $\gamma(G)$ is strongly dependent on how the inputs and outputs are scaled. The minimized scaled condition number $\gamma^*(G)$ is obtained by minimizing $\gamma(S_1 GS_2)$ over all possible input and output scalings, S_1 and S_2. There is a very close relationship between γ^* and the absolute sum of the elements in the RGA; $\|\Lambda\|_1 = \Sigma_{i,j}|\lambda_{ij}|$. For 2×2 plants (Nett and Manousiouthakis, 1987; Grosdidier *et al.*, 1985)

$$\|\Lambda\|_1 - \frac{1}{\gamma^*(G)} \leqslant \gamma^*(G) \leqslant \|\Lambda\|_1. \quad (18)$$

Consequently, for 2×2 plants the difference between these quantities is at most one and $\|\Lambda\|_1$ approaches $\gamma^*(G)$ as $\gamma^*(G) \to \infty$. Since $\|\Lambda\|_1$ is much easier to compute than $\gamma^*(G)$, it is the preferred quantity to use.

3.3. *The RGA and input uncertainty (Skogestad and Morari, 1987d)*

Again, consider uncertainty on the plant inputs as given by (12). The loop transfer matrix, G_pC, for the perturbed plant may be written in terms of its nominal value, GC:

$$G_pC = GC(I + C^{-1}\Delta_IC). \quad (19)$$

G_pC is closely related to performance because of (15). For 2×2 plants the error term $C^{-1}\Delta_IC$ in (19) may be expressed in terms of the RGA of the controller

$$C^{-1}\Delta_IC =$$

$$\begin{bmatrix} \lambda_{11}(C)\Delta_1 + \lambda_{21}(C)\Delta_2 & \lambda_{11}(C)\dfrac{c_{12}}{c_{11}}(\Delta_1 - \Delta_2) \\ -\lambda_{11}(C)\dfrac{c_{21}}{c_{22}}(\Delta_1 - \Delta_2) & \lambda_{12}(C)\Delta_1 + \lambda_{22}(C)\Delta_2 \end{bmatrix} (20)$$

If any element in $C^{-1}\Delta_IC$ is large compared to 1, the loop transfer matrix G_pC is likely to be very different from the nominal (GC) and poor performance or even instability is expected when $\Delta_I \neq 0$. Controllers with large RGA-elements should generally be avoided, because otherwise the closed-loop system is very sensitive to input uncertainty (Skogestad and Morari, 1987d).

It should be added that it is the behavior of G_pC at frequencies close to the closed-loop bandwidth (where $\sigma_i(G_pC) \approx 1$) which is of primary importance for the stability of the closed-loops system. Therefore, it is particularly bad if the controller has large RGA-elements in this frequency range.

Inverse-based controller. To have "tight" control it is desirable to use an inverse-based controller $C(s) = c(s)G^{-1}(s)$ where $c(s)$ is a scalar. In this case $GC = cI$ and $G_pC = c(I + C^{-1}\Delta_IC)$ and performance is clearly going to be poor when the controller has large RGA-elements. Furthermore, since $\Lambda(C) = \Lambda(G^{-1}) = \Lambda^T(G)$, the controller will have large RGA-elements whenever the plant has. Consequently, inverse-based controllers should *never* be used for plants with large RGA-elements. In particular, this applies to LV-control of high-purity distillation columns which always yields large RGA-elements.

Control of plants with large RGA-elements. We clearly should not use an inverse-based controller for a plant with large RGA-elements. On the other hand, a diagonal controller is insensitive to uncertainty $(C^{-1}\Delta_IC = \Delta_I)$, but is not able to correct for the strong directionality of the plant, which implies that performance has to be sacrificed. This is confirmed by the results presented below.

4. FORMULATION OF THE CONTROL PROBLEM

4.1. *Performance and uncertainty specifications*

The uncertainty and performance specifications are the same as those used by Skogestad and Morari (1986).

Uncertainty. The only source of uncertainty considered is uncertainty on the manipulated inputs (L and V) with a magnitude bound

$$w_I(s) = 0.2 \frac{5s + 1}{0.5s + 1}. \tag{21}$$

The possible perturbed plants G_p are obtained by allowing any $dL = dL_c(1 \pm |w_I|)$ and $dV = dV_c(1 \pm |w_I|)$. (Actually, the perturbations are allowed to be complex, mainly for mathematical convenience). (21) allows for an input error of up to 20 % at low frequency as is used in the simulations (9). The uncertainty in (21) increases with frequency. This allows, for example, for a time delay of about 1 min in the response between the inputs, L and V, and the outputs, y_D and x_B. In practice, such delays may be caused by the flow dynamics. Therefore, although flow dynamics are not included in the models or in the simulations, they are partially accounted for in the μ-analysis and in the controller design.

Performance. Robust performance is satisfied if

$$\bar{\sigma}(S_p) = \bar{\sigma}((I + G_pC)^{-1}) \leqslant \frac{1}{|w_P|} \tag{15}$$

is satisfied for all possible plants, G_p. We use the performance weight

$$w_P(s) = 0.5 \frac{10s + 1}{10s}. \tag{22}$$

A particular S which exactly matches the bound (15) at low frequencies and satisfies it easily at high frequencies is $S = 20s/20s + 1$. This corresponds to a first-order response with closed-loop time constant 20 min.

4.2. *Analysis of controllers*

Comparison of controllers is based mainly on computing μ for robust performance (μ_{RP}). Simulations are used only to support conclusions found using the μ-analysis. The main advantage of using the μ-analysis is that it provides a well-defined basis for comparison. On the other hand, simulations are strongly dependent on the choice of setpoints, uncertainty, etc.

The value of μ_{RP} is indicative of the worst-case response. If $\mu_{RP} > 1$ then the "worst case" does not satisfy our performance objective, and if $\mu_{RP} < 1$ then the "worst case" is better than required by our performance objective. Similarly, if $\mu_{NP} < 1$ then the performance objective is satisfied for the *nominal* case. However, this may not mean very much if the system is sensitive to uncertainty and μ_{RP} is significantly larger

than one. We will show below that this is the case, for example, if an inverse-based controller is used for our distillation column.

4.3. *Controllers*

We will study the distillation column using the following six controllers:

(1) Diagonal PI-controller.

$$C_{PI}(s) = \frac{0.01}{s} (1 + 75s) \begin{pmatrix} 2.4 & 0 \\ 0 & -2.4 \end{pmatrix}. \tag{23}$$

This controller was studied in Skogestad and Morari (1986) and it was tuned in order to achieve as good a performance as possible while maintaining robust stability.

(2) Steady-state decoupler plus two PI-controllers [i.e. the inverse of the crude model (7)].

$$C_{0inv}(s) = 0.7 \frac{(1 + 75s)}{s} G^S(0)^{-1}$$

$$= \frac{0.01(1 + 75s)}{s} \begin{pmatrix} 27.96 & -22.04 \\ 27.60 & -22.40 \end{pmatrix}. \tag{24}$$

This controller was tuned to achieve good *nominal* performance. However, the *controller* has large RGA-elements ($\lambda_{11}(C) = 35.1$) at *all* frequencies and we expect the controller to be extremely sensitive to input uncertainty.

(3) Inverse-based controller based on the linear model $G_1^S(s)$ for Case 1.

$$C_{1inv}(s) = \frac{0.7}{s} G_1^S(s)^{-1}. \tag{25}$$

At low frequency this controller is equal to $C_{0inv}(s)$. Note that $C_{1inv}(s)$ and $G_1^S(s)^T$ have the same RGA-elements. Therefore from Fig. 2 we expect $C_{1inv}(s)$ to be sensitive to input uncertainty at low frequency, but not at high frequency.

(4, 5 and 6) μ-optimal controllers based on the models $G_0(s)$, $G_1(s)$ and $G_2(s)$. The controllers are denoted $C_{0\mu}(s)$, $C_{1\mu}(s)$ and $C_{2\mu}(s)$, respectively and their state–space descriptions are given in Appendix.

These controllers were obtained by minimizing $\sup_\omega \mu(N_{RP})$ for each model using the input uncertainty and performance weights given above. The numerical procedure used for the minimization is the same as outlined in Skogestad and Morari (1986). The μ-plots for RP for the μ-optimal controllers are of particular interest since they indicate the best *achievable* performance for the plant. Bode-plots of the transfer matrix elements for $C_{1\mu}(s)$ and $C_{2\mu}(s)$ are shown in Fig. 4. Note the similarities between these controllers and the simple diagonal PI-controller (23).

At low frequency ($s \rightarrow 0$) the six controllers are

A: $C_{1\mu}(s)$

B: $C_{2\mu}(s)$
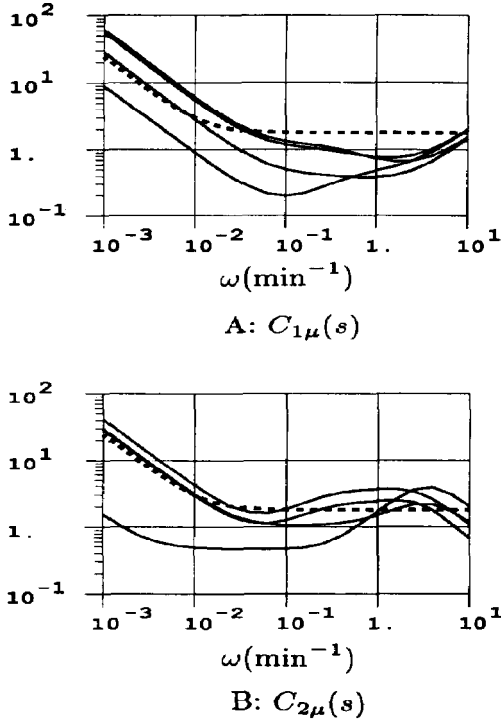
Fig. 4. Magnitude plots of elements in μ-optimal controllers $C_{1\mu}(s)$ and $C_{2\mu}(s)$. Dotted line: $C_{PI}(s)$.

approximately

$$C_{PI} = \frac{0.01}{s}\begin{pmatrix} 2.4 & 0 \\ 0 & -2.4 \end{pmatrix}$$

$$C_{0inv} = C_{1inv} = \frac{0.01}{s}\begin{pmatrix} 27.96 & -22.04 \\ 27.80 & -22.40 \end{pmatrix}$$

$$C_{0\mu} = \frac{0.01}{s}\begin{pmatrix} 3.82 & -0.92 \\ 1.73 & -3.52 \end{pmatrix}$$

$$C_{1\mu} = \frac{0.01}{s}\begin{pmatrix} 6.07 & -0.90 \\ 2.80 & -2.93 \end{pmatrix}$$

$$C_{2\mu} = \frac{0.01}{s}\begin{pmatrix} 4.06 & +0.15 \\ 2.85 & -2.93 \end{pmatrix}.$$

The value of $\|\Lambda(C)\|_1$ as a function of frequency is shown for the six controllers in Fig. 5. As expected, the μ-optimal controllers have small RGA-elements, which make them insensitive to the input uncertainty. For example, $C_{2\mu}$ is nearly triangular at low frequency and consequently has $\Lambda \approx I$.

5. RESULTS FOR OPERATING POINT A

In this section we will study how the six controllers perform at the nominal operating point A for the three assumptions regarding condenser and reboiler holdup [corresponding to the models $G_1(s)$, $G_2(s)$ and $G_3(s)$]. The μ-plots for the 18 possible combinations are given in Fig. 6. The upper solid line is $\mu(N_{RP})$ computed from (16). The lower solid line is $\mu(N_{NP}) = \bar{\sigma}((I + GC)^{-1})$.

1: $C_{PI}(s)$
2: $C_{0inv}(s)$
3: $C_{1inv}(s)$
4: $C_{0\mu}(s)$
5: $C_{1\mu}(s)$
6: $C_{2\mu}(s)$
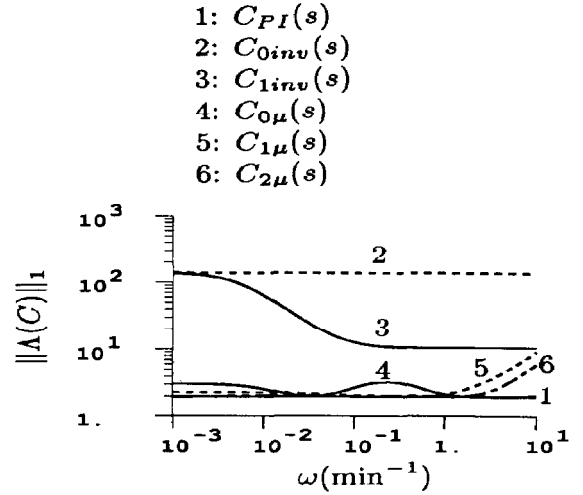
Fig. 5. Magnitude of RGA-elements of controllers. $\|\Lambda(C)\|_1 = \sum_{i,j}|\lambda_{ij}(C)|$.

The dotted line is $\mu(N_{RS})$ [eq. (14)]. A number of interesting observations can be derived from these plots. These are presented below. In some cases the simulations in Figs 7–9 are used to support the claims.

5.1. Discussion of controllers

$C_{PI}(s)$. The simple diagonal PI-controller performs reasonably well in all cases. μ_{NP} is higher than one at low frequency, which indicates a slow return to steady-state. This is confirmed by the simulations in Fig. 8 for a feed rate disturbance; after 200 min the column has still not settled. Operators are usually unhappy about this kind of response. The controller is insensitive to input uncertainty and to changes in reboiler and condenser holdup.

$C_{0inv}(s)$. This controller uses a steady-state decoupler. The nominal response is very good for Case 1 (Fig. 7), but the controller is extremely sensitive to input uncertainty. In practice, this controller will yield an unstable system (Skogestad and Morari, 1986).

$C_{1\ inv}(s)$. This controller is based on the model $G_1(s)$ and therefore gives an excellent nominal response for Case 1 (Fig. 6). This is also confirmed by the simulations in Fig. 7; the response is almost perfectly decoupled with a time constant of about 1.4 min. Since the simulations are performed with the full-order model, while the controller was designed based on the simple two time-constant model, $G_1(s)$ (8), this confirms that $G_1(s)$ yields a very good approximation of the linearized plant when the reboiler and condenser holdups are small. The controller is sensitive to the input uncertainty as expected from the RGA-analysis. Also note that the controller performs very poorly when the condenser and reboiler holdups are increased. This shows that the controller is very sensitive also to other sources of model–plant mismatch.
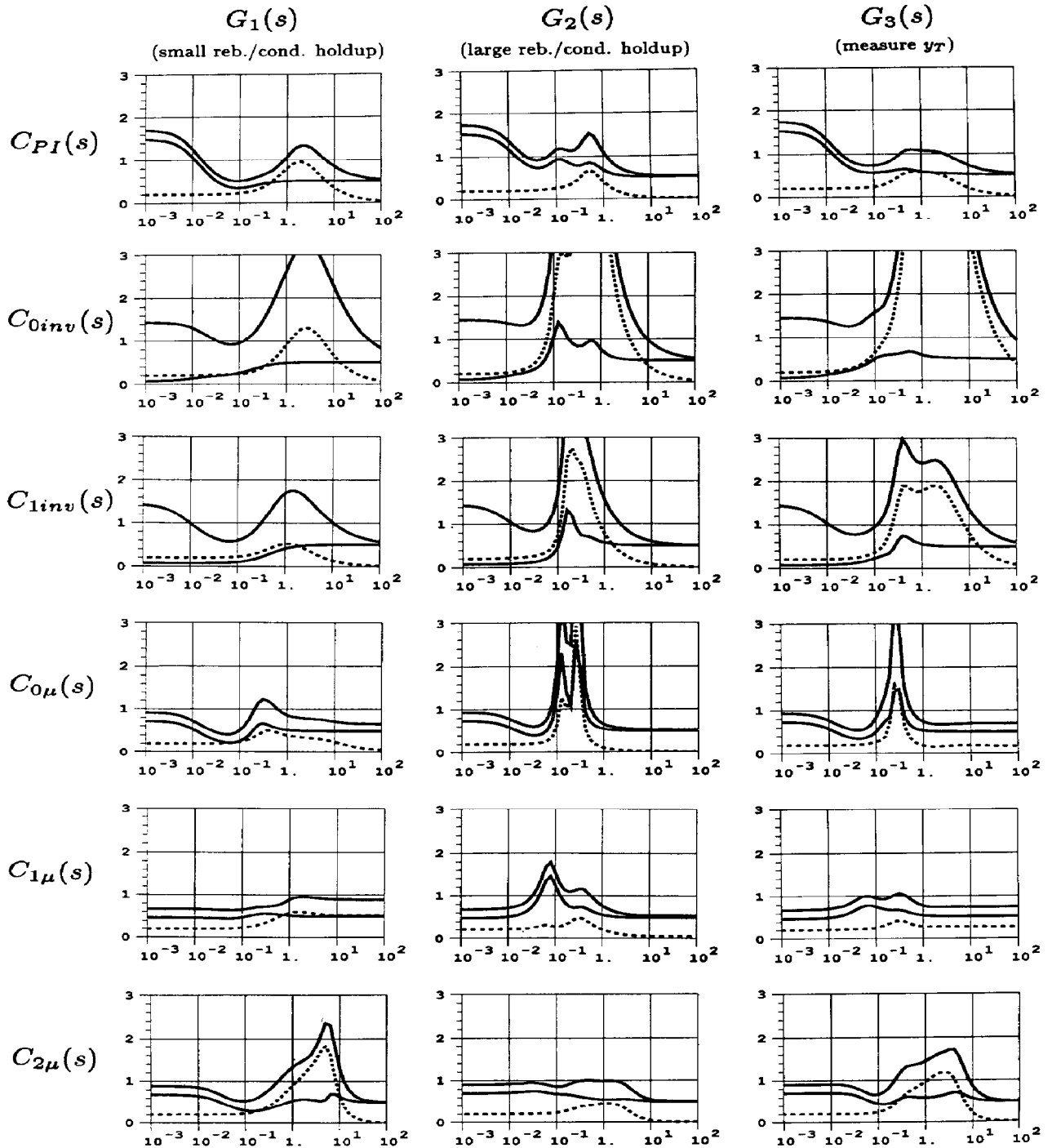
Fig. 6. μ-plots of Column A. Upper solid line: $\mu(N_{RP})$ for robust performance; lower solid line: $\mu(N_{NP})$ for nominal performance; dotted line: $\mu(N_{RS})$ for robust stability. The RP-, NP- or RS-requirement is satisfied if the corresponding μ-curve is less than one at all frequencies.

$C_{0\mu}(s)$. This is the μ-optimal controller from our previous study (Skogestad and Morari, 1986) which was designed based on the very simplified model $G_0(s)$. The controller performs surprisingly well on the actual plant $(G_1(s))$ when the holdups are negligible.

However, the controller is seen to perform very poorly when the holdup in the reboiler and condenser is increased, which shows that the controller is very sensitive to other sources of model inaccuracies (for which it was not designed).
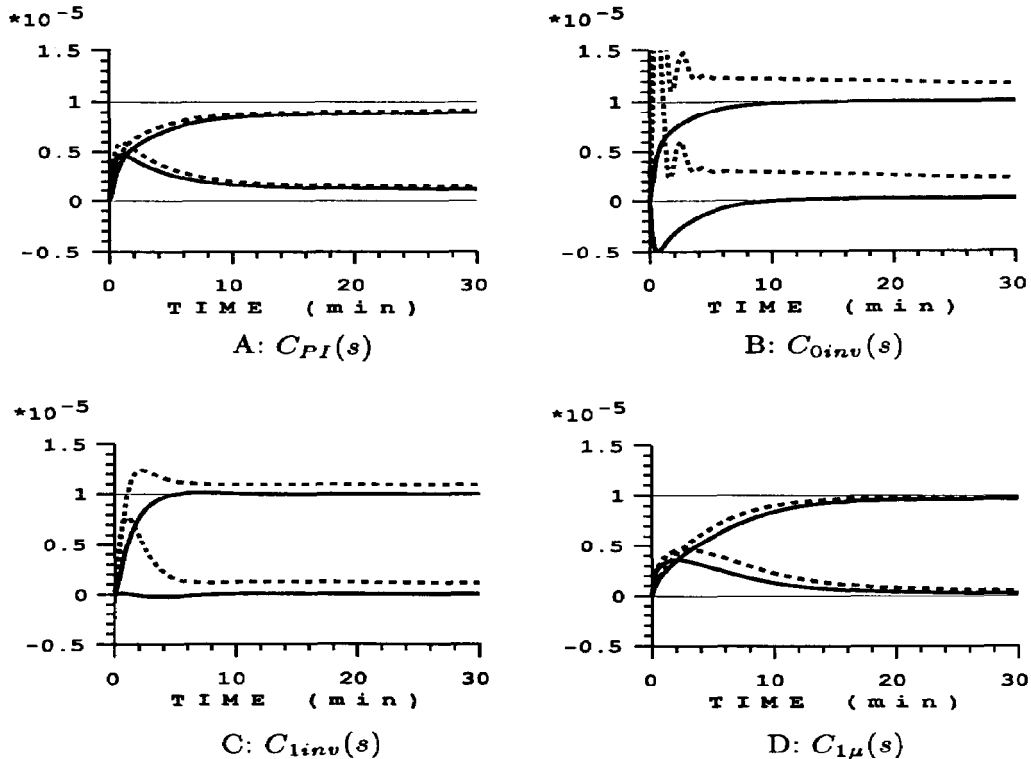
Fig. 7. Column A, Case 1. Closed-loop response to small setpoint change in y_D. Solid lines: no uncertainty; dotted lines: 20% uncertainty on inputs L and V (eq. 9).
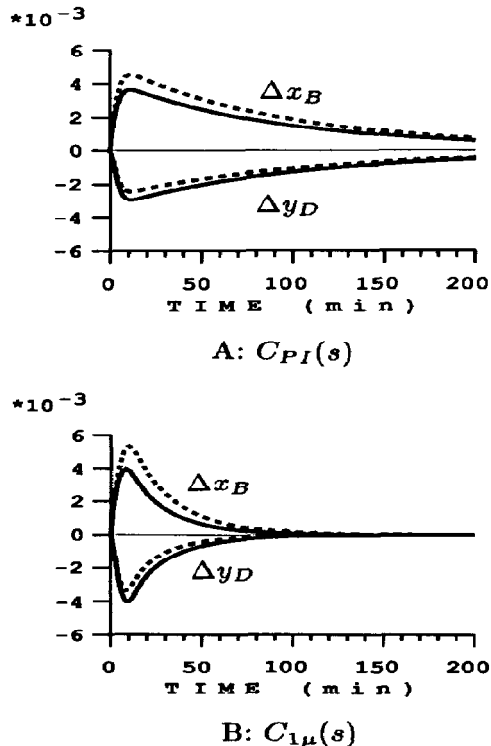
Fig. 8. Column A, Case 1. Closed-loop response to a 30% increase in feed rate. Solid lines: no uncertainty; dotted lines: 20% uncertainty on inputs L and V (eq. 9).

$C_{1\mu}(s)$. This is the μ-optimal controller when there is negligible holdup $(G_1(s))$, and the RP-condition is satisfied for this case since $\mu_{RP} \approx 0.95$. The nominal performance is not as good as for the inverse-based controller $C_{1inv}(s)$; we have to sacrifice nominal performance to make the system robust with respect to uncertainty. The controller shows some performance deterioration when the reboiler and condenser holdups are increased (Case 2). This is not surprising since the added holdup makes the response in y_D and x_B more sluggish; the open- loop response for y_D changes from approximately $1/1 + 194s$ to $1/(1 + 194s)(1 + 10s)$ (recall discussion following (8)]. As expected, the controller is much less sensitive to changes in condenser holdup if overhead composition is measured in the vapor line (Case 3). Overall, this is the best of the six controllers.

$C_{2\mu}(s)$. This is the μ-optimal controller for the case with considerable reboiler and condenser holdup, and with y_D measured in the condenser $(G_2(s))$. $\mu_{RP} \approx 1.00$ for this case. The nominal response is good in all cases (Fig. 6), but the controller is very sensitive to uncertainty when the plant is $G_1(s)$ or $G_3(s)$ rather than $G_2(s)$. This is clearly not desirable since changes in condenser and reboiler holdup are likely to occur during normal operation. The observed behavior is not surprising since the controller includes lead elements at $\omega \approx 0.1$ (Fig. 4B) to counteract the lags caused by the reboiler and condenser holdups. If these lags are not

Case 1   Case 2

(small reb./cond. holdup)   (large reb./cond. holdup)
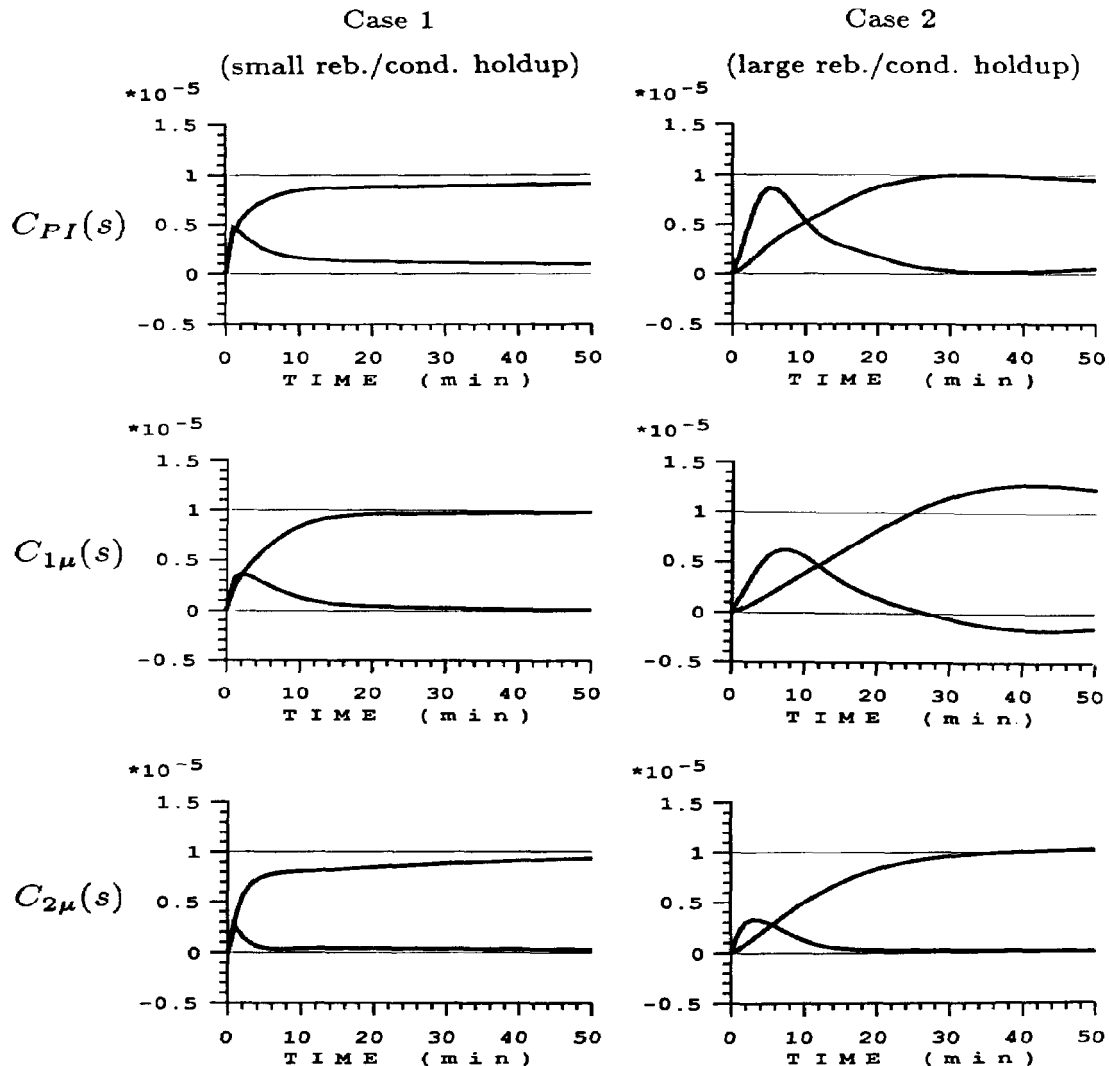
Fig. 9. Column A. Effect of reboiler and condenser holdup on closed-loop response. No uncertainty.

present in the plant $[G_1(s)$ or $G_3(s)]$, the "derivative" action caused by the lead elements result in a system which is very sensitive to uncertainty.

5.2. Conclusions

—The μ-optimal controller $C_{0\mu}(s)$ applied to the plant $G_0(s)$ yields $\mu_{RP} \approx 1.06$ (Skogestad and Morari, 1986), while the μ-optimal controller $C_{1\mu}(s)$ applied to the plant $G_1(s)$ yields $\mu_{RP} \approx 0.95$. Thus, somewhat surprisingly, the achievable performance is not much better for $G_1(s)$ than for $G_0(s)$, even though $G_0(s)$ is ill-conditioned and has large RGA-elements at *all* frequencies, while $G_1(s)$ only has large RGA-elements at low frequencies (Fig. 1). This seems to indicate that large RGA-elements at low frequency imply limitations on the achievable control performance and partially justifies the use of steady-state

values of the RGA for selecting the best control configuration (Shinskey, 1984).

—However, the use of the more detailed model $G_1(s)$, rather than $G_0(s)$, is still justified since the resulting μ-optimal controller is much less sensitive to changes in reboiler and condenser holdup (which will occur during operation).

—The two time-constant model $G_1(s)$ approximates the full-order model very closely as seen from Fig. 7C; the response is almost perfectly decoupled when there is no uncertainty.

—To avoid sensitivity to the amount of condenser and reboiler holdup, the overhead composition should be measured in the overhead vapor, rather than in the condenser. In practice, temperature measurements *inside* the column are often used to infer compositions, and the dynamic response of these measurements is similar to that when the condenser and reboiler holdup is neglected.

—The simple model $G_2(s)$ is useful for controller design also when the reboiler and condenser holdup is large.

—The main advantage of the μ-optimal controllers over the simple diagonal PI-controller is a faster return to steady-state. This comes out very clearly in Fig. 8 which shows the closed-loop response to a 30% increase in feed rate.

—Strictly speaking, it is the peak value of $\mu(N_{RP})$ for robust performance which should be considered. However, additional insight may be gained by studying $\mu(N_{RP})$ as a function of frequency. A small (large) value of $\mu(N_{RP})$ at low frequency generally implies a fast (slow) return to steady state. Similarly, a small (large) value of $\mu(N_{RP})$ at high frequency implies a good (poor) initial response. These interpretations become clear by comparing the first column of the μ-plots in Fig. 6 with the corresponding simulations in Fig. 7.

6. EFFECT OF NONLINEARITY (RESULTS FOR OPERATING POINT C)

In this paper we do not treat nonlinearity as uncertainty as was attempted in Skogestad and Morari (1986). The reason is that this approach is not rigorous and is also easily very conservative because of the strong correlation between all the parameters in the model which is difficult to account for. Furthermore, we know from the insights presented by Skogestad and Morari (1987a) that the column is actually *not* as nonlinear as one might expect. Though the steady-state gains may change dramatically, the *initial response* (the high frequency behavior), which is of principal importance for feedback control, is much less affected. In particular, this is the case if relative (logarithmic) compositions are used (Skogestad and Morari, 1987a). To demonstrate this we compute μ and show simulations for some of the controllers when the "plant" is $G_C^S(s)$ rather than $G^S(s)$.

6.1. Modelling

$G_C(s)$ corresponds to the same column as $G(s)$, but the distillate flow rate (D/F) has been increased from 0.5 to 0.555 such that $y_D = 0.9$ and $x_B = 0.002$ (see Table 1). For Case 1 $(M_D/F = M_B/F = 0.5$ min), the following approximate model is derived when scaled compositions $(dy_D/0.1, dx_B/0.002)$ are used:

$$G_{C1}^S(s) = \begin{pmatrix} \dfrac{16.0}{1+\tau_1 s} & \dfrac{-16.0}{1+\tau_1 s} + \dfrac{0.023}{1+\tau_2 s} \\ \dfrac{9.3}{1+\tau_1 s} & \dfrac{-9.3}{1+\tau_1 s} - \dfrac{1.41}{1+\tau_2 s} \end{pmatrix} \qquad (27)$$

with $\tau_1 = 24.5$ min and $\tau_2 = 10$ min.

The steady-state gains and time constants are entirely different from those at operating point $A(8)$. Also note that at steady state $\lambda_{11}(G(0)) = 35.1$ for Column A, but only 7.5 for Column C. However, at high frequency the scaled plants at operating points A and C

are very similar. (8) and (27) yield:

$$G_1^S(\infty) = \frac{1}{s}\begin{pmatrix} 0.45 & -0.36 \\ 0.56 & -0.65 \end{pmatrix} \quad \lambda_{11}(\infty) = 3.2 \quad (28a)$$

$$G_{C1}^S(\infty) = \frac{1}{s}\begin{pmatrix} 0.65 & -0.65 \\ 0.38 & -0.52 \end{pmatrix} \quad \lambda_{11}(\infty) = 3.7. \quad (28b)$$

Therefore, as we will show, controllers which were designed based on the model $G^S(s)$ (operating point A) do in fact perform satisfactory also when the plant is $G_C^S(s)$ rather than $G^S(s)$. Recall that the use of a scaled plant is equivalent to using logarithmic compositions $(Y_D$ and $X_B)$. The variation in gains with operating conditions is much larger if unscaled compositions are used—both at steady-state (Table 1) and at high frequencies:

$$G_1(\infty) = \frac{0.01}{s}\begin{pmatrix} 0.45 & -0.36 \\ 0.56 & -0.65 \end{pmatrix} \qquad (29a)$$

$$G_{C1}(\infty) = \frac{0.01}{s}\begin{pmatrix} 6.5 & -6.5 \\ 0.08 & -0.10 \end{pmatrix}. \qquad (29b)$$

6.2. μ-Analysis

The μ-plots with the model $G_C^S(s)$ and four of the controllers are shown in Fig. 10 (all four controllers yield *nominally* stable closed-loop systems). At high frequencies the μ-values are almost the same as those found at operating point A. The only exception is the inverse-based controller $C_{1inv}(s)$ which was found to be robustly stable at operating point A, but which is not at operating point C. Again, this confirms the sensitivity of this controller to model inaccuracies. Performance is clearly worse at low frequencies at operating point C (Fig. 10) than at operating point A (Fig. 6). This is expected; the controllers were designed based on model A, and the plants are quite different at low frequencies.

The μ-optimal controller $C_{1\mu}(s)$ satisfies the robust performance requirements also at operating point C when the reboiler and condenser holdups are small. Consequently, with the use of scaled (logarithmic) compositions, a single linear controller is able to give acceptable performance at these two operating points which have quite different linear models. The main difference between $C_{1\mu}(s)$ and the diagonal PI-controller is again that the μ-optimal controller gives a much faster return to steady-state. This is clearly seen from Fig. 11A.

6.3. Logarithmic versus unscaled compositions

Figure 10 shows how controllers designed based on the *scaled* plant $G^S(s)$ at operating point A, perform for the *scaled* plant (different scaling factors!) at operating point C; this is equivalent to using logarithmic compositions $(Y_D$ and $X_B)$. However, we know from (29) that the plant model shows much larger changes if absolute (unscaled) compositions $(y_D$ and $x_B)$ are used. We therefore expect the closed-loop performance to be entirely different at operating points A and C when unscaled (absolute) compositions are used. This is indeed confirmed by Fig. 11B which shows the closed-

$$G_{C1}(s)$$

(small reb./cond. holdup)

$$G_{C2}(s)$$

(large reb./cond. holdup)

$C_{PI}(s)$

$C_{1inv}(s)$

$C_{1\mu}(s)$

$C_{2\mu}(s)$
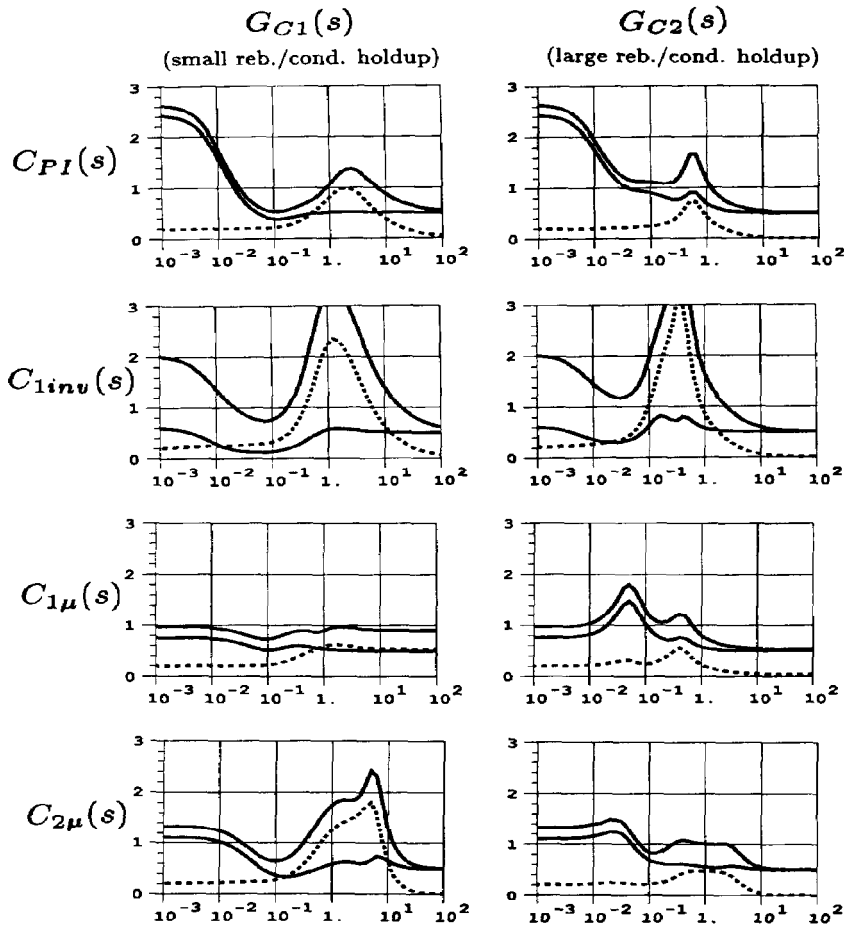
Fig. 10. μ-Plots for column C. Upper solid line: $\mu(N_{RP})$; lower solid line: $\mu(N_{NP})$; dotted line: $\mu(N_{RS})$.

loop response to a small setpoint change in x_B at operating point C. Fig. 11B should be compared to Fig. 11A which shows the same response, but using logarithmic compositions as controlled outputs. In Fig. 11B (absolute compositions) the response for x_B is significantly more sluggish and the response for y_D is much faster than in Fig. 11A (logarithmic compositions). This is exactly what we would expect by comparing (29a) and (29b): The high-frequency gain for changes in y_D is increased by an order of magnitude and the gain for changes in x_B is reduced by an order of magnitude. However, recall from (28) that the gain shows very small changes if logarithmic compositions are used.

The simulations in Fig. 12 are with no flow dynamics and in practice we expect the system to be *unstable* at operating point C if unscaled (absolute) compositions are used; the loop gain for y_D is increased by a factor of about 10 compared to the design conditions at operating point A. This conclusion is supported by the following analysis: Assume we use the diagonal controller $C_{PI}(s)$ and are only controlling top composition (y_D) using reflux (L). Then the analysis reduces to a SISO-problem. At operating point A the loop transfer

function for this loop is (unscaled compositions)

$$A: \quad g_{11}c(s) = \frac{0.878}{1 + 194s} \frac{2.4(1 + 75s)}{s}.$$

This corresponds to a closed-loop bandwidth $(|g_{11}c(j\omega_c)| \approx 1)$ of about $\omega_c \approx 0.81$ min^{-1}. The phase of $g_{11}c$ at this frequency is about $-90°$C. The system will therefore become unstable if $90° = \pi/2$ rad additional phase lag is added at this frequency. Consequently, the maximum allowed deadtime is $\theta_{max} = 1.57/0.81 = 1.93$ min. Next, consider operating point C

$$C: \quad g_{11}c(s) = \frac{1.6}{1 + 24.5s} \frac{2.4(1 + 75s)}{s}.$$

Here $\omega_c \approx 11.7$ min^{-1} and the phase is again about $-90°$. This gives a maximum allowed deadtime of only $\theta_{max} = 1.57/11.7 = 0.13$ min. There may not actually be deadtime in the system, but the presence of other sources of phase lag (valve dynamics, measurements dynamics, etc.) will most certainly result in an unstable system.

$$C_{1\mu}(s) \quad \text{- - -} \quad C_{PI}(s)$$
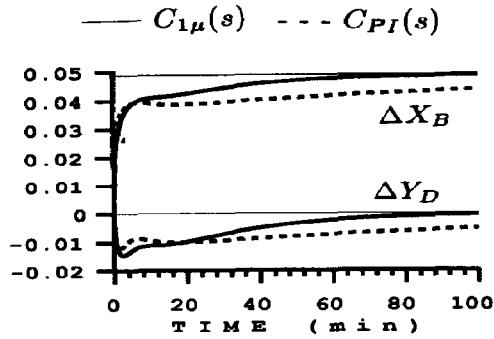
A: Logarithmic compositions
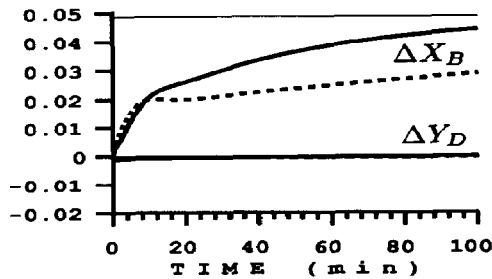
B: Absolute compositions

Fig. 11. Column C, Case 1. Closed-loop response to small setpoint change in x_B (x_B increases from 0.002 to 0.0021) using diagonal PI-controller (dotted line) and the μ-optimal controller for column A (solid line). (A) Logarithmic compositions as controlled outputs (equivalent to using scaled compositions); (B) absolute (unscaled) compositions as controlled outputs. No uncertainty.

$$\text{---} \quad C_{1\mu}(s)$$

$$\text{- - -} \quad C_{PI}(s)$$
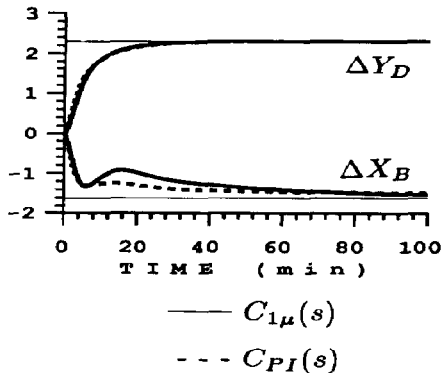
Fig. 12. Transition from operating point A to C (Case 1) using controllers $C_{1\mu}$ (solid line) and C_{PI} (dotted line). Logarithmic compositions are used as controlled outputs to reduce the effect of nonlinearity. Desired trajectory is a first-order response with time constant 10 min. No uncertainty.

6.4. Transition from operating point A to C

Figure 12 shows a transition from operating point A ($Y_D = X_B = 4.605$) to operating point C ($Y_D = 2.303$, $X_B = 6.215$) using logarithmic compositions as controlled outputs. The desired setpoint change is a first

order response with time constant 10 min:

$$\Delta Y_{D_r} = \frac{2.303}{1 + 10s}, \quad \Delta X_{B_r} = \frac{-1.609}{1 + 10s}.$$

The closed-loop response is seen to be very good. The diagonal controller $C_{PI}(s)$ and the μ-optimal controller $C_{1\mu}(s)$ give very similar responses in this particular case. (However, the μ-optimal controller generally performs better at operating point C as is evident from Fig. 10 and 11.) This illustrates that a linear controller, based on the nominal operating point A, can perform satisfactory for large deviation from this operating point when logarithmic compositions are used.

7. CONCLUSIONS

A single linear controller is able to give satisfactory control of this high-purity column at widely different operating conditions. One reason for this is the use of logarithmic compositions which effectively counteracts the nonlinearity in the plant. However, even if a absolute compositions are used, a single linear controller performs satisfactory if the deviations from steady-state are reasonably small.

Using the composition in the overhead vapor, y_T, as a controlled output makes the system less sensitive to variations in the condenser holdup.

A simple diagonal controller was found to be robust with respect to model–plant mismatch, but gives a sluggish return to steady-state. This particular part of the response is improved using the μ-optimal controller. Inverse-based controllers, and in particular those based on a steady-state decoupler, are very sensitive to model–plant mismatch and should not be used with the LV-configuration for this high-purity column.

NOTATION (ALSO SEE FIG. 1)

$G(s)$ linear transfer function model of plant

$C(s)$ linear controller

$\bar{\sigma}(G)$ maximum singular value of G corresponding to the maximum 2-norm gain at each frequency

$$\bar{\sigma}(G) = \max_{u \neq 0} \frac{\|Gu\|_2}{\|u\|_2} (j\omega)$$

$$\|u\|_2 = \sqrt{\sum_i |u_i|^2} \quad (2\text{---norm of vector } u)$$

$\underline{\sigma}(G)$ minimum singular value of G corresponding to the minimum 2-norm gain at each frequency

$$\underline{\sigma}(G) = \min_{u \neq 0} \frac{\|Gu\|_2}{\|u\|_2} (j\omega)$$

$\gamma(G)$ $= \bar{\sigma}(G)/\underline{\sigma}(G)$ condition number of G

$\gamma^*(G)$ $= \min_{S_1, S_2} \gamma(S_1 G S_2)$ minimum condition number of G (S_1 and S_2 are diagonal "scaling" matrices with real, positive entries)

$\Lambda(G) = \{\lambda_{ij}\} = G \times (G^{-1})^T$ relative gain array (RGA) of matrix G ($\times$ denotes element-by-element multiplication, also called the Schur or Haddemard product)

$\|\Lambda\|_1 = \sum_{i,j} |\lambda_{ij}|$ 1-norm (sum of element magnitudes) of matrix Λ

$\mu(N)$ structured singular value of matrix N (Doyle, 1982)

Subscripts

0   crude model (7) of column
1,2   cases for condenser and reboiler holdup (Section 2). 1—small holdup, 2—large holdup
3   y_T as controlled output and large holdup
C   operating point C (no subscript denotes operating point A)
p   perturbed (with input uncertainty Δ_I)
P   performance

Superscripts

S   scaled compositions (eq. 2)
o   nominal conditions

REFERENCES

Bristol, E. H., 1966, On a new measure of interactions for multivariable process control. *IEEE Trans. Aut. Control* AC-11, 133–134.

Doyle, J. C., 1982, Analysis of feedback systems with structured uncertainties. *IEE Proc.* 129, Pt. D, 6, 242–250.

Fuentes, C. and Luyben, W. L., 1983, Control of high-purity distillation columns. *Ind. Engng Chem. Proc. Des. Dev.* 22, 361–366.

Grosdidier, P., Morari, M. and Holt, B., 1985, Closed-loop properties from steady-state gain information. *Ind. Engng Chem. Fund.* 24, 221–235.

Kapoor, N., McAvoy, T. J. and Marlin, T. E., 1986, Effect of recycle structure on distillation tower time constant. *A.I.Ch.E. J.* 32, 3, 411–418.

Moczek, J. S., Otto, R. E. and Williams, T. J., 1963, Approximation model for the dynamic response of large distillation columns. *Proc. 2nd IFAC Cong.*, Basel. Also

published in *Chem. Eng. Prog. Symp. Ser.* 61, 136–146 (1965).

Moore, B. C., 1981, Principal component analysis in linear systems: Controllability, observability and model reduction. *IEEE Trans. Aut. Control.* AC-26, 17–32.

Nett, C. N. and Manousiouthakis, V., 1987, Euclidean condition number and block relative gain: connections, conjectures and clarifications. *IEEE Trans. Aut. Control.* AC-32, 405–407.

Ryskamp, C. J., 1981, Explicit versus implicit decoupling in distillation control. *Chem. Proc. Control 2nd Conference*, Sea Island, GA, 18–23 Jan. (Published in T. F. Edgar and D. E. Seborg (eds.), United Engineering Trustees (1982), available from A.I.Ch.E.

Shinskey, F. G., 1984, *Distillation Control*, 2nd Edn. McGraw-Hill, New York.

Skogestad, S. and Morari, M., 1986, Control of ill-conditioned plants: high-purity distillation", paper 74a, *A.I.Ch.E. Ann. Mtg.* Miami Beach.

Skogestad, S. and Morari, M., 1987a, Understanding the dynamic behavior of distillation columns. *Ind. Engng Chem. Res.* (in press).

Skogestad, S. and Morari, M., 1987b, Understanding the steady-state behavior of distillation columns. In preparation.

Skogestad, S. and Morari, M., 1987c, Control configurations selection for distillation columns. *A.I.Ch.E. J.* (in press).

Skogestad, S. and Morari, M., 1987d, Implications of large RGA-elements on control performance. *Ind. Engng Chem. Res.* (in press).

APPENDIX: STATE–SPACE REALIZATIONS OF PLANTS AND CONTROLLERS

Below are shown state–space realizations of $G(s) = C(sI - A)^{-1}B + D$ using "packed" form

$$\begin{bmatrix} A & B \\ C & D \end{bmatrix}$$

where D in all cases is a 2×2 matrix. The plant models and controllers are for the scaled plant, that is, correspond to using logarithmic compositions. All controllers were designed based on operating point A and when unscaled (absolute) compositions are used as controlled outputs the controllers should be multiplied by

$$\frac{1}{x_B^o} = \frac{1}{1 - y_D^o} = 100.$$

$G_1^S(s)$:

−5.155e−03	0.000e+00	7.131e−02	−7.131e−02
0.000e+00	−6.667e−02	−1.556e−17	3.762e−02
6.347e−02	2.481e−02	0.000e+00	0.000e+00
7.821e−02	−2.481e−02	0.000e+00	0.000e+00

$G_2^S(s)$:

−4.539e−03	0.000e+00	0.000e+00	0.000e+00	0.000e+00	7.110e+00	−7.105e+00
0.000e+00	−3.086e−02	0.000e+00	0.000e+00	0.000e+00	6.297e+00	−7.408e+00
0.000e+00	0.000e+00	−8.580e−02	0.000e+00	0.000e+00	5.845e+00	−2.658e+00
0.000e+00	0.000e+00	0.000e+00	−1.708e−01	0.000e+00	2.852e+00	−5.414e+00
0.000e+00	0.000e+00	0.000e+00	0.000e+00	−8.876e−01	−2.699e+00	2.872e+00
6.361e−02	−5.394e−02	−1.641e−02	2.929e−03	8.189e−03	0.000e+00	0.000e+00
6.981e−02	1.664e−02	−4.683e−02	−5.886e−02	3.864e−02	0.000e+00	0.000e+00

$G_3^S(s)$:

−4.533e−03	0.000e+00	0.000e+00	0.000e+00	0.000e+00	−6.962e−01	6.958e−01
0.000e+00	−3.184e−02	0.000e+00	0.000e+00	0.000e+00	−5.982e−01	7.055e−01
0.000e+00	0.000e+00	−8.220e−02	0.000e+00	0.000e+00	6.681e−01	−4.407e−01
0.000e+00	0.000e+00	0.000e+00	−2.302e−01	0.000e+00	3.154e−01	−5.217e−01
0.000e+00	0.000e+00	0.000e+00	0.000e+00	−2.402e+00	5.535e−01	−4.607e−01
−6.185e−01	4.041e−01	−1.063e−02	6.331e−02	6.190e−01	0.000e+00	0.000e+00
−7.118e−01	−2.025e−01	−4.653e−01	−5.940e−01	−1.601e−01	0.000e+00	0.000e+00

$G_{C1}^S(s)$:

```
-4.082e-02   0.000e+00    7.354e-01   -7.354e-01
 0.000e+00  -1.000e-01   -5.659e-17    4.052e-01
 8.902e-01   5.604e-03    0.000e+00    0.000e+00
 5.175e-01  -3.488e-01    0.000e+00    0.000e+00
```

$G_{C2}^S(s)$:

```
-1.382e-02   0.000e+00    0.000e+00    0.000e+00    0.000e+00    0.000e+00    0.000e+00    5.116e-01   -5.215e-01
 0.000e+00  -7.809e-02    0.000e+00    0.000e+00    0.000e+00    0.000e+00    0.000e+00   -1.327e+00    1.540e+00
 0.000e+00   0.000e+00   -1.328e-01   -1.876e-01    0.000e+00    0.000e+00    0.000e+00    1.894e-02    2.508e-01
 0.000e+00   0.000e+00    0.000e+00    0.000e+00   -4.435e-01   -8.790e-02    0.000e+00   -1.043e+00    1.436e+00
 0.000e+00   0.000e+00    0.000e+00    0.000e+00    8.790e-02   -4.435e-01    0.000e+00    3.310e-01   -1.313e-01
 0.000e+00   0.000e+00    0.000e+00    0.000e+00    0.000e+00    0.000e+00   -3.428e+00    1.037e+00   -9.500e-01
 5.338e-01   2.476e-01   -3.312e-02   -1.014e-01    2.864e-02   -5.006e-02   -3.055e-02    1.957e-01   -2.356e-01
 3.112e-02  -7.672e-01   -4.200e-01    8.015e-01   -2.502e-01   -1.897e-02   -2.215e-01    0.000e+00    0.000e+00
```

$G_{C3}^S(s)$:

```
-1.381e-02   0.000e+00    0.000e+00    0.000e+00    0.000e+00    0.000e+00    0.000e+00    1.334e-01   -1.360e-01
 0.000e+00  -7.975e-02    0.000e+00    0.000e+00    0.000e+00    0.000e+00    0.000e+00    9.212e-02   -1.076e-01
 0.000e+00   0.000e+00   -1.758e-01   -2.017e-01    0.000e+00    0.000e+00    0.000e+00   -6.708e-02    7.042e-02
 0.000e+00   0.000e+00    0.000e+00    0.000e+00   -4.795e-01    0.000e+00    0.000e+00    1.492e-01   -1.952e-01
 0.000e+00   0.000e+00    0.000e+00    0.000e+00    0.000e+00   -3.292e+00    0.000e+00   -1.763e-01    1.859e-01
 0.000e+00   0.000e+00    0.000e+00    0.000e+00    0.000e+00    0.000e+00   -1.118e+01    1.229e-01   -9.529e-02
-9.066e-01  -3.212e-01   -8.381e-01   -1.131e+00   -1.510e+00   -1.118e+01    1.594e+00    1.212e-01   -1.045e-01
 1.164e+01   7.279e+00   -3.346e+00    1.007e-01   -2.493e-01   -2.215e-01   -1.250e-01    0.000e+00    0.000e+00
```

$C_{PI}(s)$:

```
-1.000e-06   1.000e-02    0.000e+00    0.000e+00
 0.000e+00   0.000e+00    1.000e-02   -1.000e-06
 2.400e+00   1.800e+00    0.000e+00    0.000e+00
 0.000e+00   0.000e+00   -1.800e+00   -2.400e+00
```

$C_{0inv}(s)$:

```
-1.000e-06   0.000e+00    3.994e-01   -3.149e-01
 0.000e+00  -1.000e-06    3.943e-01   -3.200e-01
 0.000e+00   0.000e+00    2.097e+01   -1.653e+01
 6.999e-01   6.999e-01    2.070e+01   -1.680e+01
```

$C_{1inv}(s)$:

```
-1.000e-06   0.000e+00    0.000e+00    0.000e+00   -3.647e+00   -4.618e+00
 0.000e+00  -1.000e-06    0.000e+00    0.000e+00    4.201e+00    4.175e+00
 0.000e+00   0.000e+00   -1.000e+03    0.000e+00   -4.066e+02   -5.200e+02
 0.000e+00   0.000e+00    0.000e+00   -1.000e+03   -4.786e+02   -4.705e+02
 5.015e-01   6.167e+01    6.167e+01   -6.249e+01    0.000e+00    0.000e+00
 5.015e-01   6.176e+01    6.176e+01   -6.112e+01    0.000e+00    0.000e+00
```

$C_{0\mu}(s)$:

-1.002e-07	0.000e+00	0.000e+00	0.000e+00	0.000e+00	0.000e+00	-6.513e-01	-9.009e-01
0.000e+00	-3.272e-06	0.000e+00	0.000e+00	0.000e+00	0.000e+00	7.224e-01	9.031e-01
0.000e+00	0.000e+00	-1.510e-01	0.000e+00	0.000e+00	0.000e+00	5.492e-02	-4.394e-02
0.000e+00	0.000e+00	0.000e+00	-9.032e+00	0.000e+00	0.000e+00	-9.086e-01	-1.136e+00
0.000e+00	0.000e+00	0.000e+00	0.000e+00	-5.838e+02	0.000e+00	1.867e+01	-1.494e+01
0.000e+00	0.000e+00	0.000e+00	0.000e+00	0.000e+00	-5.868e+02	6.722e+00	8.403e+00
6.564e-01	7.171e-01	4.949e+00	5.033e+00	-1.691e+03	-3.112e+02	5.866e+01	-3.816e+01
6.555e-01	5.425e-01	4.941e+00	-5.040e+00	-1.689e+03	3.116e+02	5.002e+01	-4.878e+01

$C_{1\mu}(s)$:

-9.993e-08	0.000e+00	0.000e+00	0.000e+00	0.000e+00	1.530e-02	1.328e-02
0.000e+00	-1.000e-07	0.000e+00	0.000e+00	0.000e+00	2.140e-02	-1.774e-02
0.000e+00	0.000e+00	-4.873e-01	0.000e+00	0.000e+00	5.557e-02	-3.543e-02
0.000e+00	0.000e+00	0.000e+00	-2.267e+03	0.000e+00	-7.372e+01	-9.722e+01
0.000e+00	0.000e+00	0.000e+00	0.000e+00	-3.840e+03	4.796e+01	7.539e+01
1.592e+00	1.699e+00	4.751e+00	8.698e+03	-5.536e+03	3.526e+02	4.821e+02
-1.215e+00	2.176e+00	4.566e+00	-8.566e+03	5.777e+03	-3.509e+02	-4.815e+02

$C_{2\mu}(s)$:

-9.487e-08	3.248e-09	0.000e+00	0.000e+00	0.000e+00	0.000e+00	0.000e+00	0.000e+00
-3.248e-09	-9.487e-08	0.000e+00	0.000e+00	0.000e+00	0.000e+00	0.000e+00	0.000e+00
0.000e+00	0.000e+00	-1.136e-07	0.000e+00	0.000e+00	0.000e+00	0.000e+00	0.000e+00
0.000e+00	0.000e+00	0.000e+00	-2.372e-01	0.000e+00	0.000e+00	0.000e+00	0.000e+00
0.000e+00	0.000e+00	0.000e+00	0.000e+00	-2.237e+00	1.977e+00	0.000e+00	0.000e+00
0.000e+00	0.000e+00	0.000e+00	0.000e+00	-1.977e+00	-2.237e+00	0.000e+00	0.000e+00
0.000e+00	0.000e+00	0.000e+00	0.000e+00	0.000e+00	0.000e+00	-2.757e+00	2.082e+00
0.000e+00	0.000e+00	0.000e+00	0.000e+00	0.000e+00	0.000e+00	-2.082e+00	-2.757e+00
-1.091e+00	-3.796e-01	1.952e+00	-6.232e+00	9.384e+00	-1.239e+01	1.924e+01	-2.277e+01
-1.304e+00	-5.861e-01	8.008e-01	-4.432e+00	5.591e+00	-2.126e+01	-1.687e+01	7.900e+00

-1.142e-02	2.193e-02
-4.747e-03	2.594e-02
1.350e-02	1.806e-02
8.986e-02	-4.583e-03
5.918e-01	-3.288e-01
2.734e-01	8.376e-02
4.328e-02	-7.059e-04
-3.761e-01	-1.111e+00
-9.749e-05	-1.833e-04
5.644e-05	1.060e-04